Available online at www.sciencedirect.com

ScienceDirect

Nanomedicine: Nanotechnology, Biology, and Medicine xx (2010) xxx – xxx

nanomedicine

www.nanomedjournal.com

Research Article

In vitro evaluation of novel polymer-coated magnetic nanoparticles for controlled drug delivery

Maham Rahimi, PhD[a,b], Aniket Wadajkar, MS[a,b], Khaushik Subramanian, MS[a,b], Monet Yousef, BS[a,b], Weina Cui, PhD[c], Jer-Tsong Hsieh, PhD[d,e], Kytai Truong Nguyen, PhD[a,b,*]

[a]*Joint Biomedical Engineering Program, University of Texas Southwestern Medical Center at Dallas, Dallas, Texas, USA and University of Texas at Arlington, Arlington, Texas, USA*

[b]*Department of Bioengineering, University of Texas at Arlington, Arlington, Texas, USA*

[c]*Department of Radiology, University of Texas Southwestern Medical Center at Dallas, Dallas, Texas, USA*

[d]*Department of Urology, University of Texas Southwestern Medical Center at Dallas, Dallas, Texas, USA*

[e]*Graduate Institute of Cancer Biology, China Medical University, Taichung, Taiwan*

Received 15 September 2009; accepted 25 January 2010

Abstract

Previously uncharacterized poly(*N*-isopropylacrylamide-acrylamide-allylamine)-coated magnetic nanoparticles (MNPs) were synthesized using silane-coated MNPs as a template for radical polymerization of *N*-isopropylacrylamide, acrylamide, and allylamine. Properties of these nanoparticles such as size, biocompatibility, drug loading efficiency, and drug release kinetics were evaluated in vitro for targeted and controlled drug delivery. Spherical core-shell nanoparticles with a diameter of 100 nm showed significantly lower systemic toxicity than did bare MNPs, as well as doxorubicin encapsulation efficiency of 72%, and significantly higher doxorubicin release at 41°C compared with 37°C, demonstrating their temperature sensitivity. Released drugs were also active in destroying prostate cancer cells (JHU31). Furthermore, the nanoparticle uptake by JHU31 cells was dependent on dose and incubation time, reaching saturation at 500 μg/mL and 4 hours, respectively. In addition, magnetic resonance imaging capabilities of the particles were observed using agarose platforms containing cells incubated with nanoparticles. Future work includes investigation of targeting capability and effectiveness of these nanoparticles in vivo using animal models.

Key words: Magnetic nanoparticles; Temperature-responsive polymers; Prostate cancer; Doxorubicin

Magnetic nanoparticles (MNPs) coated with temperature-sensitive polymers have been attracting great attention because of their various applications in the fields of biotechnology and medicine. In particular, temperature-sensitive coated MNPs have been used extensively in controlled and targeted drug release systems.[1-4] These nanocomposites are superior to the traditional stimuli-responsive systems such as pH and temperature-sensitive polymers, because they offer the advantage of noncontact force (e.g., an external magnetic field).[4,5] The external magnetic field is used to guide nanocomposites to a disease site and induce heat as a stimulus to the polymer shell.[4,6-8] These magnetic targeted carriers have also been designed with dual functionality as imaging agents and drug carriers.[5] In general, these systems are capable of site-specific targeting and controlled and sustained drug release with high biocompatibility because of the reduction in systemic toxicity.[9,10]

Of these temperature-sensitive polymer-coated MNPs, poly-(*N*-isopropylacrylamide) (PNIPAAm)-coated MNPs are of particular interest because of their stimuli (temperature) responsiveness and enhanced drug-loading ability.[11,12] These characteristics are due to their large inner volume, amphiphilicity, capacity for manipulation of permeability, and response to an external temperature stimulus with an on-off mechanism.[6,11,12]

Financial support was provided by U.S. Department of Defense Idea Development Award W81XWH-09-1-0313 (K.N.), Flight Attendants Medical Research Institute (J-T.H), and the Small Animal Imaging Resource Program (U24 CA126608) and the Biological Threat Reduction Program (P41-RR02584) to W.C.

*Corresponding author: 501 West First Street, ELB 220, Arlington, Texas 76019, USA.

E-mail address: knguyen@uta.edu (K.T. Nguyen).

1549-9634/$ – see front matter © 2010 Elsevier Inc. All rights reserved.
doi:10.1016/j.nano.2010.01.012

However, one potential problem with using PNIPAAm as a polymer coat is that its lower critical solution temperature (LCST), the temperature at which a phase transition occurs, is below body temperature (32°C). To increase the LCST of PNIPAAm above body temperature, it has been co-polymerized with different monomers, such as acrylamide (AAm).[13-15] To increase the site-specific targeted capability of PNIPAAm-AAm, it is necessary to incorporate monomers consisting of functional groups such as amine for conjugation of antibodies specific for target cells. Functionalization of the polymer would introduce impurities and change the LCST dramatically. Therefore, there is a need to suitably functionalize the nanoparticles without changing the LCST. It has been shown that polymerization of PNIPAAm with allylamine (AH) has an insignificant effect in change of the LCST of the PNIPAAm polymer.[16] Furthermore, the presence of amine groups in AH would provide more sites for bioconjugation. Therefore, it is more advantageous to polymerize PNIPAAm with both AAm and AH, because this co-polymer would increase the LCST above body temperature and provide amine groups for conjugation of bioactive molecules.

We have recently developed a process for covalently coating MNPs with PNIPAAm and PNIPAAm-AAm-AH.[8,17] We have shown that these previously uncharacterized PNIPAAm-AAm-AH-coated MNPs have a LCST above body temperature and functional groups on their surface for conjugation of biomolecules.[18] In this research we intend to investigate the in vitro characteristics of our nanoparticles for drug delivery applications. To manufacture the PNIPAAm-AAm-AH-coated MNPs, two synthetic steps were used. First, MNPs were covalently bound with a silane coupling agent, vinyltrimethoxysilane (VTMS), to produce a template site for a radical polymerization. NIPA, AAm, and AH were then polymerized on the silicon layer around the MNPs via methylene-bis-acrylamide and ammonium persulfate as a cross-linking agent and an initiator, respectively. The nanoparticle size and morphology were analyzed using transmission electron microscopy (TEM). The biocompatibility of the synthesized nanoparticles against fibroblast cells was studied using lactate dehydrogenase (LDH) assays. The drug release behavior of doxorubicin (DOX, an anticancer drug model) from the nanoparticles at temperatures below and at the LCST was also analyzed. Furthermore, the pharmacological activity of drug-loaded nanoparticles on prostate cancer cells (JHU31) was determined using cell proliferation (e.g., MTS) assays. Additionally, we performed prostate cancer cellular uptake studies of these nanoparticles via iron assays to determine the optimal dosage and incubation time. Confocal microscopy was also used to observe the location of our nanoparticles once inside prostate cancer cells. Finally, magnetic resonance imaging (MRI) studies were performed to determine the imaging capability of these nanoparticles. Being able to monitor the location of the drug-loaded nanoparticles after administration proved to be a considerable advantage in cases such as cancer therapy, in which the drug has serious side effects on healthy tissues.[19] Furthermore, it would be possible to image the cancer in vivo and discern the effect of the therapy on the tumor.[20] This type of multifunctionality (ability to image and provide therapy) in MNPs has recently been gaining interest.[21]

Methods

Materials

Ferric chloride hexahydrate and ferrous chloride tetrahydrate were purchased from Fluka (Buchs, Switzerland). Sodium hydroxide (NaOH), sodium dodecyl sulfate (SDS), docusate sodium salt, ammonium persulfate, *N*,*N*,*N*,*N*-tetramethylethylenediamine (TEMED), methylene-bis-acrylamide (BIS), VTMS, acetic acid, ethanol, AAm, AH, *N*-hydroxysuccinimide (NHS), 1-ethyl-3-(3-dimethylaminopropyl) carbodiimide hydrochloride (EDC), NIPA, and agarose were purchased from Sigma-Aldrich (St. Louis, Missouri) and used as received. Mounting medium and bovine antibody to rabbit IgG–Texas Red were purchased from Santa Cruz Biotechnology (Santa Cruz, California). Cells (i.e., NIH 3T3 fibroblast and JHU31 prostate cancer cell lines) were obtained from American Type Culture Collection (ATCC, Manassas, Virginia), and cell culture media and supplements were purchased from Invitrogen (Carlsbad, California).

Preparation of magnetic nanoparticles

MNPs were manufactured by a conventional co-precipitation method as described previously.[8] In brief, ferric chloride hexahydrate and ferrous chloride tetrahydrate (2:1) were dissolved in 600 mL of deionized (DI) water. After purging the solution with argon gas, 0.36 g of docusate sodium salt in 16 mL of hexane was added as a surfactant, and the solution was heated to 85°C. At this temperature, 7.1 M NaOH was added. After a 2-hour reaction period, particles were washed extensively with ethanol and then centrifuged at 25,000 rpm for 45 minutes. The MNPs were dried in a vacuum oven.

Preparation of VTMS-coated MNPs

The MNPs were coated with VTMS via acid catalyst hydrolysis, followed by electrophilic substitution of ferrous oxide on the surface of MNPs as shown in our previous study.[8] In brief, 0.487 mL of VTMS was hydrolyzed using 3 mL of acetic acid in the presence of water and ethanol (1:100 vol/vol). A measured quantity (0.074 g) of MNPs was then dispersed by sonication at 100 W for 30 minutes in this solution. After 24 hours of vigorous mechanical stirring at room temperature (23-25°C), VTMS-coated MNPs were obtained, excessively washed with a mixture of water and ethanol (1:100 vol/vol), and collected using an external magnet. The particles were dispersed in water before the next step.

Immobilization of PNIPAAm-AAm-AH on the surface of MNPs

VTMS-coated MNPs were used as a template to polymerize PNIPAAm-AAm-AH in an aqueous micellar solution. SDS and BIS were used as surfactant and as cross-linking agent, respectively, as previously described with a small modification.[8,17,22] In brief, 0.028 g of VTMS-coated MNPs, 0.1 g of NIPA, 0.0129 g of AAm, 0.0345 mL of AH, 0.0131 g of BIS, and 0.041 g of SDS were sonicated in 100 mL cold water for 30 minutes. Then, 0.078 g of ammonium persulfate and 101 μL of TEMED were added to the solution, and the reaction was carried out at room temperature under argon gas for 4 hours. The product

was purified several times with DI water by using a magnet to collect only PNIPAAm-AAm-AH-coated MNPs. PNIPAAm-AAm-coated MNPs and PNIPAAm-coated MNPs were also formulated using the same synthesis process as with PNIPAAm-AAm-AH-coated MNPs, but without addition of AH and without addition of both AH and AAm monomers, respectively.

TEM studies

TEM (JEOL 1200 EX; JEOL, Tokyo, Japan) was used to determine the size and core-shell structure of PNIPAAm-AAm-AH-coated MNPs. In general, nanoparticle samples were prepared by drop-casting an aqueous dispersion of nanoparticles onto a carbon-coated copper grid, and the grid was dried at room temperature before viewing under the microscope. The nanoparticles were stained with phosphotungstic acid at a concentration of 0.01% (vol/vol) before analysis.

Nanoparticle biocompatibility

To assess the biocompatibility of PNIPAAm-AAm-AH-coated MNPs, the cytotoxicity was tested by measuring LDH released from damaged cells after exposure to these nanoparticles. Fibroblast cells (NIH 3T3) were cultured to confluence, harvested by trypsinization, and dispersed in Dulbecco's minimal essential medium supplemented with 10% serum and 1% penicillin-streptomycin. Cells were seeded at a density ~10,000 cells per well in 24-well plates and incubated for 24 hours at 37°C. Nanoparticles were then added and incubated in wells with fibroblasts for 6 and 24 hours at various concentrations (0, 16, 31, 62, 125, 250, and 500 μg/mL). Two types of nanoparticles were used for this study: the original MNPs and PNIPAAm-AAm-AH-coated MNPs. LDH released in medium from damaged cells was analyzed using an LDH Assay (Promega, Madison, Wisconsin), following the manufacturer's instructions.

Drug loading

For drug-loading and drug release studies, DOX was used as a model drug. In brief, 10 mg of freeze-dried PNIPAAm-AAm-AH-coated MNPs and 5 mg of DOX were dispersed in phosphate buffer solution (PBS). The solution was stirred at 4°C for 3 days. The DOX-loaded PNIPAAm-AAm-AH-coated MNPs were separated from the solution using an external magnet. The solution was then analyzed using an ultraviolet-visible (UV-Vis) spectrofluorometer (Infinite M200 plate reader; Tecan, Durham, North Carolina) to determine the amount of unencapsulated DOX (λ_{ex} 470 nm and λ_{em} 585 nm). This value was then compared to the total amount of added DOX to determine the DOX-loading efficiency of the nanoparticles. Loading efficiency was calculated according to the following formula:

$$\text{Loading Efficiency} = \frac{\text{Total [DOX] used} - \text{unencapsulated [DOX]}}{\text{Total [DOX] used}} \times 100\%$$

In vitro drug release kinetics

To study the drug release profile of synthesized PNIPAAm-AAm-AH-coated MNPs, drug-loaded nanoparticles dispersed in PBS as described earlier were placed inside dialysis bags with a molecular weight cutoff (MWCO) of 10,000 Da. Samples were incubated at various temperatures: 4°C, 37°C, and 41°C. At designated time intervals, 1 mL of dialysate was removed from each sample and stored at –20°C for later analysis. Dialysate volume was reconstituted by adding 1 mL of fresh PBS to each sample. After the experiment the dialysate samples were analyzed using a UV-Vis spectrofluorometer (Tecan) to determine the amount of DOX released into the dialysate (λ_{ex} 470 nm and λ_{em} 585 nm for DOX measurement).

Pharmacological activity of DOX-loaded PNIPAAm-AAm-AH-coated MNPs

To investigate the pharmacological activity of DOX released from our nanoparticles, cancer cell viability was conducted using MTS assays (Promega) according to the manufacturer's instructions. JHU31 cells were cultured to confluence, harvested by trypsinization, and dispersed in RPMI medium supplemented with 10% (vol/vol) serum and 1% (vol/vol) penicillin-streptomycin. Cells were seeded at a density of approximately 10,000 cells per well in 24-well plates for 24 hours at 37°C. Cells were then incubated with either nanoparticles, DOX-loaded nanoparticles, or free DOX. The concentration of nanoparticles and DOX-loaded nanoparticles was 500 μg/mL. We selected this nanoparticle concentration according to drug release results from our nanoparticles and the optimal inhibition dose of DOX on JHU31 cell growth studies. The cells were incubated with each group at 37°C, 41°C, and temperature cycles between 37°C and 41°C (1 hour at each temperature for one cycle) for 24 hours. After the incubation period, cells in each group were processed to MTS assays for cell viability.

Cellular uptake studies of PNIPAAm-AAm-AH-coated MNPs

To characterize in vitro behavior of our nanoparticles uptaken by JHU31 cells, cellular uptake studies were performed. Cells were seeded at a density of ~10,000 cells per well in 24-well plates and allowed to adhere and grow for 24 hours at 37°C. To investigate effects of the nanoparticle optimal dosage and incubation time, PNIPAAm-AAm-AH-coated MNPs were added at various concentrations (0, 125, 250, 300, 500, 800, and 1000 μg/mL) to the cell-seeded wells and incubated for 6 hours. After the incubation period, cells were lysed with 1% Triton X-100 in PBS. To test for the optimal incubation time, 500 μg/mL of PNIPAAm-AAm-AH-coated MNPs were added to a 24-well plate and incubated for varying durations (0, 0.5, 1, 2, 4, 6, and 8 hours). At predetermined time intervals, the cells were lysed with 1% Triton X-100 in PBS.

To determine the amount of iron uptake, we performed an iron content assay as previously described.[23] In brief, 500 μL of cell lysate were incubated in 30% (vol/vol) hydrochloric acid at 55°C for 2 hours, and then 0.05 mg of ammonium persulfate was added. After shaking for 15 minutes, 50 μL of a 0.1 M solution of potassium thiocyanate were added and the samples shaken for another 15 minutes. These samples were read for absorbance using a UV-Vis spectrophotometer (Tecan) at 478 nm to determine the amount of iron in our samples, which correlates with the iron uptake within the cells. The cell lysate was also

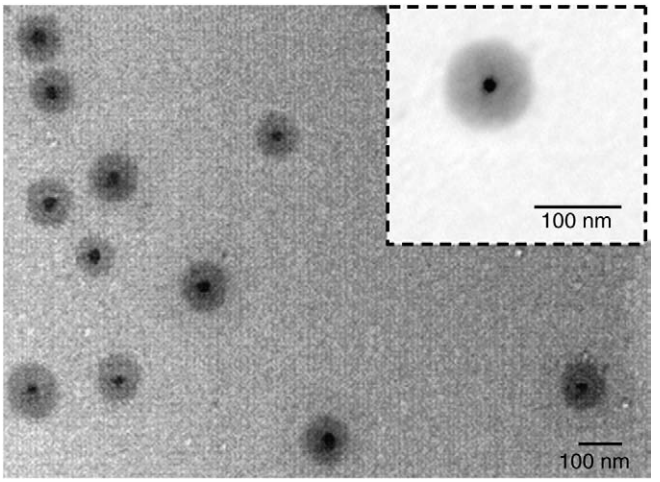

Figure 1. Transmission electron micrograph of PNIPAAm-AAm-AH coated magnetic nanoparticles (inset is a higher magnification image).

analyzed for the total DNA content using a Picogreen DNA Assay (Invitrogen), and these data were used to normalize the iron content.

To visualize the uptake of PNIPAAm-AAm-AH-coated MNPs, Texas Red (bovine antibody to rabbit IgG–Texas Red) was conjugated to our nanoparticles via carbodiimide chemistry. In brief, 0.01 g of PNIPAAm-AAm-AH-coated MNPs was dissolved in 0.5 mL of 2-(N-morpholino)ethanesulfonic acid (MES) (0.1 M) buffer solution, and 0.01 g of each, NHS and EDC, were added. The reaction was mixed for 10 minutes at room temperature, after which 0.2 mg of Texas Red was added to the above solution and the reaction stirred vigorously for 2 hours at room temperature under dark conditions. To remove unreacted Texas Red the product was washed and purified several times with DI water using an external magnet.

MRI studies of prostate cancer cells loaded with PNIPAAm-AAm-AH-coated MNPs

Prostate cancer cells were cultured and grown to confluence as described above. The confluent cell culture was incubated with a 300-μg/mL concentration of the PNIPAAm-AAm-AH-coated MNPs for 3 hours. Following incubation, the cells were washed three times with fresh medium. After trypsinization the cells were suspended in 10 mL Dulbecco's minimal essential medium and centrifuged for 10 minutes at 1000 rpm. The resultant pellet was then resuspended in 10 mL fresh medium to make a stock cell suspension. To prepare the agarose platform for MRI study, agarose was added to a 0.9% (wt/vol) sodium chloride solution and was heated to 100°C to ensure complete melting. After cooling the stock agarose solution to 37°C, a cell suspension was added with the agarose solution to reach a final cell concentration of 10^6 cells/mL and an agarose concentration of 1% (wt/vol) in the test tube (a total volume of 10 mL), and the solution was allowed to cool to room temperature. Control agarose platform is the 1% agarose without cells. MR images were obtained for the agarose platform controls and samples using a Varian unity INOVA 4.7T 40-cm horizontal MR system equipped with actively shielded gradients (Varian, Palo Alto, California) (205 mm with 22G/cm). The sample was put into a home-built 35-mm volume radiofrequency coil. Multislice T_2-weighted images (TR = 2000 msec; TE = 15 msec; field of view of 30 mm × 30 mm; matrix = 128 × 128; slice thickness = 2 mm) were acquired with spin echo pulse sequence.

Results

Size, morphology, and core-shell structure of nanoparticles

The average size of the synthesized PNIPAAm-AAm-AH-coated MNPs was analyzed using TEM. We have previously investigated synthesized MNPs and silane-coated MNPs.[8] The synthesized PNIPAAm-AAm-AH-coated MNPs were ~100 nm in diameter as shown in Figure 1. The image also reveals the core (dark center) of magnetic nanoparticles and the shell structure of the coated polymer (surrounding penumbra).

Nanoparticle biocompatibility

LDH cell viability assay was used to investigate the biocompatibility of PNIPAAm-AAm-AH-coated MNPs along with bare MNPs as control by quantifying the LDH released from damaged fibroblasts after exposure to these nanoparticles. Results from the LDH assay after 6 hours of nanoparticle exposure showed that the presence of bare MNPs at low concentrations ranging from 16 to 31 μg/mL reduced the cell viability by less than 20% (Figure 2). However, further increase in concentrations resulted in a significant drop in cell viability by as much as 62% for a concentration of 500 μg/mL. Bare MNPs present after a 24-hour incubation period showed significantly higher cytotoxicity as compared with those present after a 6-hour incubation—even at a low concentration of 31 μg/mL. In contrast to the bare MNPs, the PNIPAAm-AAm-AH-coated MNPs showed much less toxicity with cell viability greater than 80% when incubated with particles for 24 hours, including those at high concentrations (Figure 2).

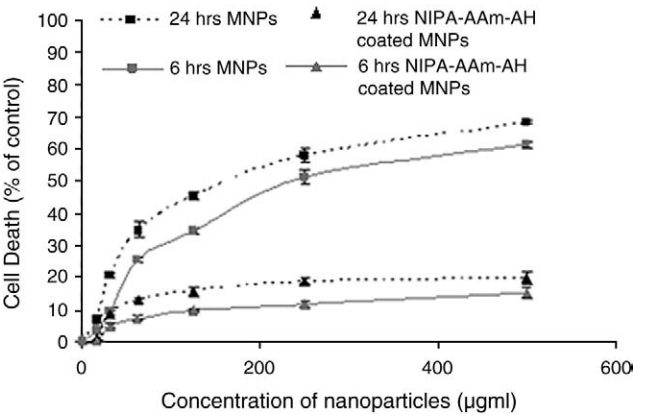

Figure 2. Cytotoxicity study of magnetic nanoparticles (MNPs) and PNIPAAm-AAm-AH coated MNPs on fibroblasts. Cells treated with 1% Triton X-100 were used as a positive control (100% cytotoxicity).

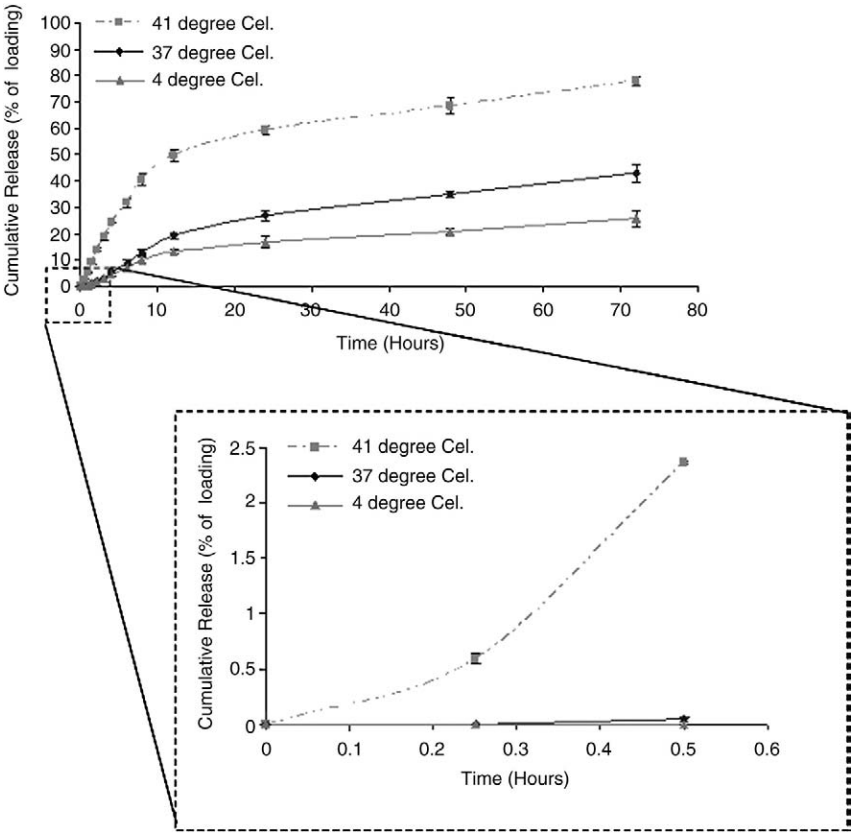

Figure 3. In vitro release profiles of doxorubicin (DOX) at 4°C, 37°C, and 41°C. Cumulative percentage release of DOX over 72 hours. The inset is the cumulative percentage release of DOX over 30 minutes.

Drug-loading efficiency and release kinetics

The loading efficiency of DOX-loaded PNIPAAm-AAm-AH-coated MNPs was determined according to the formula illustrated earlier in the Methods section. The results indicated that ~72% of the incubated DOX was loaded into the PNIPAAm-AAm-AH-coated MNPs, similar to other studies,[20,21] in which a hydrophilic drug was loaded into PNIPAAm-based MNPs. The release behavior of the nanoparticles was studied for ~72 hours in PBS (0.1 M, pH 7.4) at 4°C, 37°C, and 41°C. The percentage of cumulative release of DOX at 41°C was significantly higher than at 4°C and 37°C (Figure 3).

Pharmacological activity of DOX-loaded PNIPAAm-AAm-AH-coated MNPs

To investigate the pharmacological activity of the released drugs from our nanoparticles, the viability of JHU31 cells exposed to DOX-loaded nanoparticles was assessed. As shown in Figure 4, *A*, the free DOX decreased cell viability to 20% in comparison with the control, whereas DOX-loaded nanoparticles decreased cell viability to 70% at 37°C. However, when cells were exposed at 41°C or temperature cycles between 37°C and 41°C (1 hour each at each temperature for 24 hours), DOX-loaded nanoparticles could decrease the cell viability to 12% or 36%, similar to those of free DOX, respectively (Figure 4, *B* and *C*).

Cellular uptake studies

To determine the optimal concentration of nanoparticles and the optimal incubation time required for an effective treatment, the cellular uptake of PNIPAAm-AAm-AH-coated MNPs by the prostate cancer cells was investigated. The uptake of PNIPAAm- and PNIPAAm-AAm-coated MNPs was also studied for comparison. As shown in Figure 5, *A*, JHU31 cells took up polymer-coated MNPs in a manner that was dependent on both concentration and incubation time. The highest cellular uptake was observed when the cells were treated with PNIPAAm-AAm- and PNIPAAm-AAm-AH-coated MNPs. The lowest uptake was observed when cells were treated with PNIPAAm-coated MNPs. The cellular uptake of PNIPAAm-coated MNPs formed a plateau at 300 μg/mL, whereas the cellular uptake of PNIPAAm-AAm-coated and PNIPAAm-AAm-AH-coated MNPs formed a plateau at 500 μg/mL. The incubation time studies indicated that each of the polymeric-coated MNPs reached a plateau after 4 hours (Figure 5, *B*).

To image the cellular uptake of PNIPAAm-AAm-AH-coated MNPs, Texas Red was conjugated to nanoparticles, and they were incubated with JHU31 cells for 1 hour. The results indicated that nanoparticles were internalized by the cells and accumulated in the cytoplasm (Figure 6). The success of Texas Red antibody conjugation also suggests that our nanoparticles have the functional amine groups for conjugation of biomolecules.

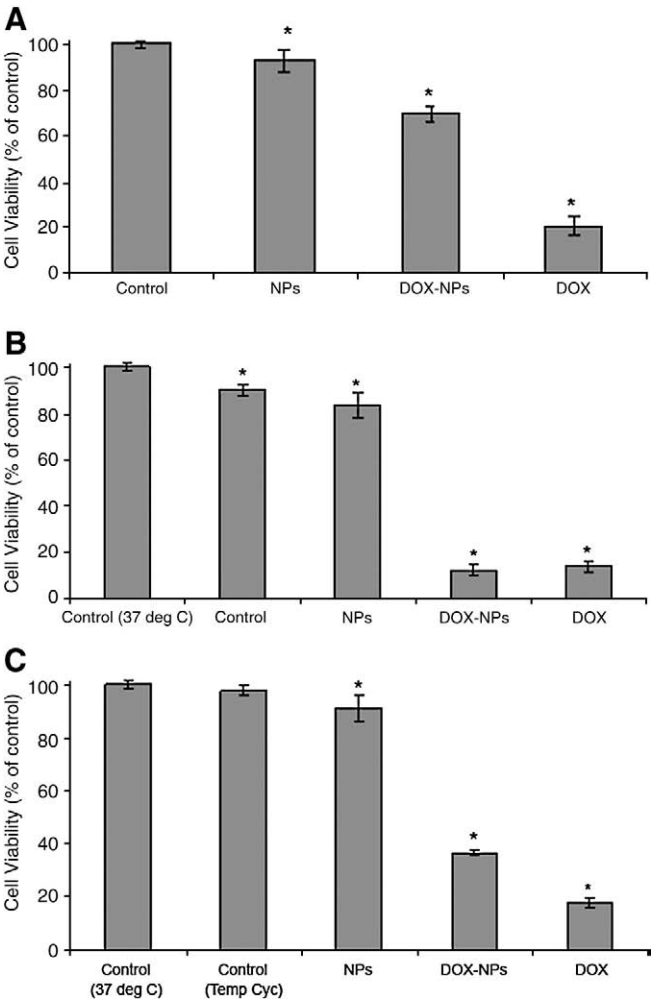

Figure 4. Pharmacological activity of doxorubicin (DOX)-loaded PNIPAAm-AAm-AH coated magnetic nanoparticles (DOX-NPs) in comparison with empty nanoparticles (NPs) and free DOX (DOX) in prostate cancer cells JHU31. The cell viability was investigated using MTS assays at **(A)** 37°C, **(B)** 41°C, and **(C)** temperature cycles between 37°C and 41°C.

Imaging capacity of the PNIPAAm-AAm-AH-coated MNPs

In Figure 7, *A* the MR imaging was carried out using JHU31 cells loaded with PNIPAAm-AAm-AH-coated MNPs. A dispersed stronger signal was observed when the cells were incubated with PNIPAAm-AAm-AH-coated MNPs (Figure 7, *A*) compared with the control preparation of agarose medium (Figure 7, *B*), which has a uniform signal distribution. The dispersed signal might be due to an excessive concentration of cells engulfing the PNIPAAm-AAm-AH-coated MNPs.

Discussion

In this work we have characterized in vitro behavior of PNIPAAm-AAm-AH-coated MNPs for targeted and controlled drug delivery applications. These nanoparticles are to our knowledge unique, in that they consist of a new temperature-sensitive polymer shell that has the LCST above body temperature and contains functional groups on their surface for bioconjugation. The polymeric shell consists of a copolymer of NIPA, AAm, and AH. The PNIPAAm-AAm-AH is polymerized onto the surface of the MNPs via a silane coupling agent and a free-radical polymerization. The size and morphology of the synthesized nanoparticles were analyzed by TEM. In addition, in vitro behaviors such as toxicity, drug-loading efficiency, drug release profile, pharmacological activity, and cellular uptake of the manufactured nanoparticles were assessed. Moreover, the MR imaging capabilities of the particles was explored. The results are discussed in detail below.

TEM was carried out to study the size, morphology, and core-shell structure of the nanoparticles. A close examination of the TEM image (inset in Figure 1) reveals the presence of MNPs (~10 nm diameter) at the center with a PNIPAAm-AAm-AH coating surrounding them. The size of the magnetic core was similar to earlier reported values of MNPs synthesized by similar methods.[8,17,24] In comparison to our previous study with PNIPAAm-coated MNPs,[8] there was clearly less agglomeration of MNPs in the core. This might be a result of the higher mixing capability due to utilization of a mechanical stirrer and the electrostatic charge repulsion from the amine group of AH in the

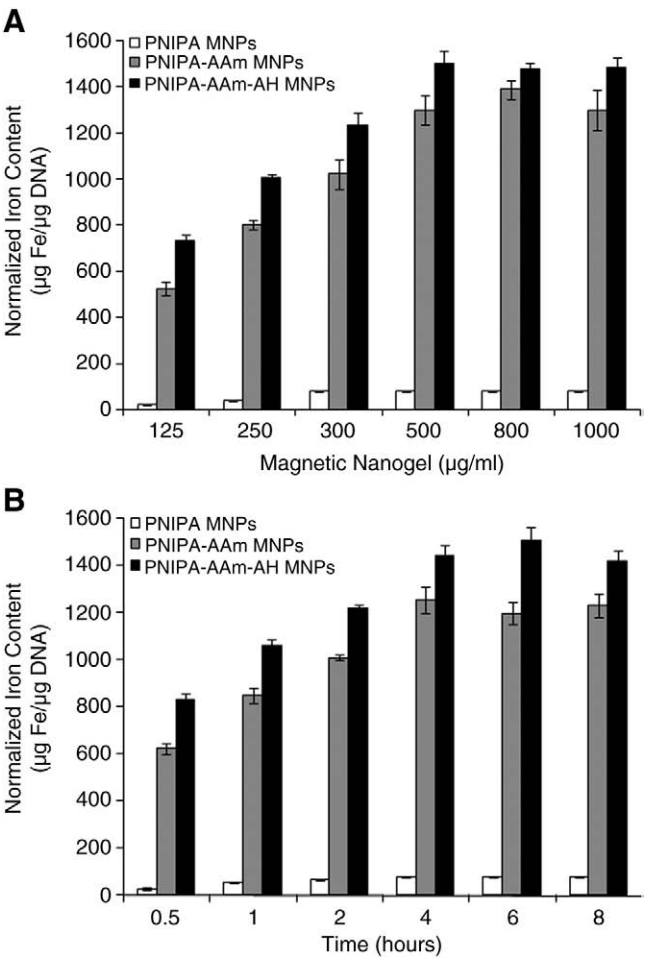

Figure 5. Cellular uptake studies. **(A)** Effects of nanoparticle concentrations on cellular uptake and **(B)** effects of incubation time on cellular uptake.

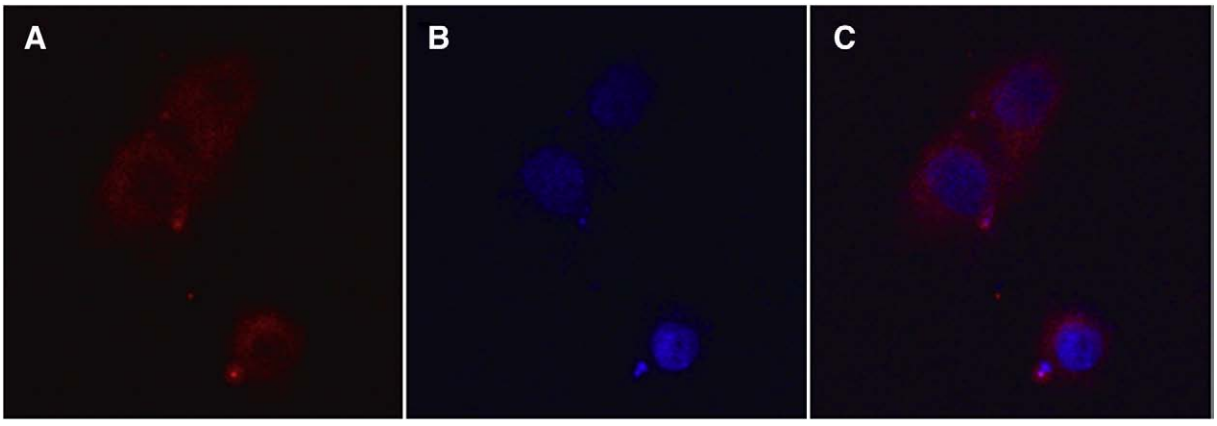

Figure 6. Uptake of nanoparticles by JHU31 prostate cancer cells using confocal microscopy. **(A)** Detection of Texas Red–conjugated nanoparticles within the cells. **(B)** Detection of nucleus (DAPI, a fluorescent stain that binds strongly to DNA). **(C)** Superimposed image of these two images.

PNIPAAm-AAm-AH coating, which would further reduce the magnetic dipole interactions and promote stability.[17]

The LDH assay for nanoparticle biocompatibility shows that MNPs and PNIPAAm-AAm-AH-coated MNPs possess similar cell compatibility at low concentrations (<31 μg/mL). Even at high concentrations, polymer-coated MNPs still demonstrated significant biocompatibility. Furthermore, cell viability at a longer incubation period still appeared favorable for the polymer-coated MNPs. Similar to our previous biocompatibility studies of PNIPAAm-coated MNPs,[24] we believe that coating MNPs with a biocompatible polymer is necessary when high concentrations of MNPs are used.

The drug release study indicates that the PNIPAAm-AAm-AH is a temperature-sensitive polymer, whereby at its LCST the nanoparticles go through the phase change to collapse and release more drugs. After 72 hours, 78% of the encapsulated DOX was released at 41°C, whereas at 4°C and 37°C ~26% and ~43% was released, respectively. This type of release is consistent with our previous studies,[8,17,24] which show the temperature sensitivity of PNIPAAm coated onto MNPs. The release profile of the DOX over the first 30 minutes is also shown in Figure 3. After 30 minutes the percentages of cumulative release of DOX were only 0% and 0.046% at 4°C and 37°C, respectively, whereas at 41°C it was 2.4%. The system is shown to release its payload over a short burst release period with changes in temperature. In contrast, other MNPs that make use of different polymer coatings such as poly(D,L-lactic-co-glycolic) acid show a much slower sustained release over extended periods of time.[25,26] This burst release in response to temperature indicates that such a stimuli-responsive system would prove to be a useful treatment for applications such as cancer treatment, in which aggressive release is required to combat cancer cell proliferation.

The effect of loading DOX into our nanoparticles on JHU31 cells was also studied with a promising outcome. As shown in Figure 4, the decreases in cell viability are much more significant, especially at 41°C in comparison to 37°C, which is an indication that our drug delivery system is sensitive to temperature and that the encapsulated drug is released at its LCST. These results also indicate that the released drug does not interact with the polymer, is not denatured, and is pharmacologically active. Similar to our nanoparticles, it has also been reported that DOX-loaded polymer-coated MNPs

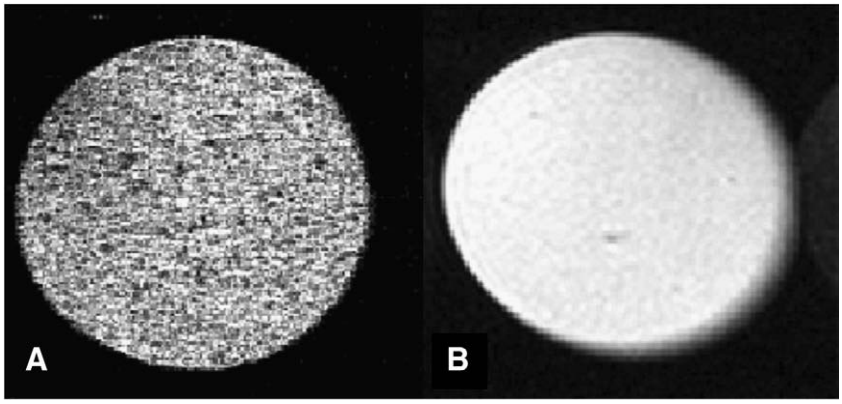

Figure 7. MR detection of prostate cancer cells JHU31 loaded with PNIPAAm-AAm-AH-coated magnetic nanoparticles (TR = 2000 msec; TE = 15 msec; in-plane resolution 230 μm × 230 μm; slice thickness = 2 mm). **(A)** Prostate cancer cells loaded with PNIPAAm-AAm-AH-coated magnetic nanoparticles. **(B)** Control (1% agarose only).

(e.g., DOX-loaded polyethylene glycol–coated MNPs) release pharmacologically active DOX with a remarkable level of cell destruction.[27]

Previous studies on cellular uptake of magnetic nanoparticles show that the uptake depends on several factors such as particle concentration, particles size, incubation time, and the type of particle coating.[28-30] Thus, cellular uptake of nanoparticles by prostate cancer cells in vitro was investigated in this study to determine the effects of these factors. Similar to other studies, we also observed the dependence on dose and incubation time in the cellular uptake of our polymer-coated MNPs. The low uptake of PNIPAAm-coated MNPs might be due to the low LCST of PNIPAAm (below incubation temperature), which results in aggregation of the nanoparticles due to hydrophobic attraction and hinders their cellular uptake. The higher threshold of particle uptake might be attributed to the elevated LCST of the PNIPAAm-AAm-coated MNPs and PNIPAAm-AAm-AH-coated MNPs, which would prevent agglomeration. Indeed, results from a particle sizer using laser scattering technology indicated that aggregation of PNIPAAm-coated MNPs at 37°C caused an eightfold increase in size, whereas PNIPAAm-AAm-coated and PNIPAAm-AAm-AH-coated MNPs remained in the original size range. Furthermore, preferential uptake of PNIPAAm-AAm-AH-coated MNPs could also be explained by the presence of electropositive amine groups on the particle surface, which would have a favorable electrostatic interaction with the negatively charged cell membrane.

Comparing the labeled cell images of Figure 7, *A* with the control of Figure 7, *B*, this result clearly shows the extremely dense concentration of the PNIPAAm-AAm-AH-coated MNPs inside the cells using MRI. The large amount of signal produced in the labeled cells might be the result of a large number of particles packed within the endocytosed vesicles within the labeled cells. An advantage of labeling prostate cancer cells with polymer-coated MNPs is that the agglomeration of particles within the endocytotic vesicles causes the nanoscale particles to act as a much larger single magnetic unit. This has two main effects: MR imaging of the tumor could be achieved at a higher resolution with regional variations of the tumor being detected,[31-33] and localized accumulation of the particles would allow for an enhanced magnetic resonance and subsequent temperature escalation.[34-37]

In this study, previously uncharacterized PNIPAAm-AAm-AH-coated MNPs were synthesized and characterized in vitro. Our results indicated that these nanoparticles consist of a core (magnetic) shell (polymer) structure with the average size of ~100 nm in diameter. LDH studies revealed that the nanoparticles were relatively biocompatible. The DOX release profiles from our nanoparticles demonstrated that our nanoparticles were sensitive to temperature with a significantly higher release at 41°C than at either 4°C or 37°C. In addition, the MTS assays indicated that the DOX released from the nanoparticles was pharmacologically active and that release was dependent on temperature. Furthermore, as a result of the properties of PNIPAAm-AAm-AH-coated MNPs, the cellular uptake of our nanoparticles was much higher than that for the PNIPAAm- and PNIPAAm-AAm-coated MNPs. The confocal images of the uptake of nanoparticles by prostate cancer cells indicated that nanoparticles accumulated mostly in the cytoplasm. MRI further supported the use of our polymer-coated MNPs for imaging and controlled drug delivery applications. In the future we will investigate the pharmacological behavior of the nanoparticles in vivo and the conjugation of specific antibodies for targeting drug delivery applications.

Acknowledgments

The TEM work was performed at the Molecular and Cellular Imaging Facility, and the MRI experiments were conducted at the Advanced Imaging Center at The University of Texas Southwestern Medical Center at Dallas.

References

1. Banerjee SS, Chen DH. Magnetic nanoparticles grafted with cyclodextrin for hydrophobic drug delivery. Chem Mater 2007;19:6345-9.
2. Jain TK, Reddy MK, Morales MA, Leslie-Pelecky DL, Labhasetwar. Biodistribution, clearance, and biocompatibility of iron oxide magnetic nanoparticles in rats. Mol Pharm 2008;5:316-27.
3. Jain TK, Richey J, Strand M, Leslie-Pelecky DL, Flask CA, Labhasetwar. Magnetic nanoparticles with dual functional properties: drug delivery and magnetic resonance imaging. Biomaterials 2008;29:4012-21.
4. Lai JJ, Hoffman JM, Ebara M, Hoffman AS, Estournès C, Wattiaux A, et al. Dual magnetic-/temperature-responsive nanoparticles for microfluidic separations and assays. Langmuir 2007;23:7385-91.
5. Hu SH, Liu TY, Liu DM, Chen SY. Nano-ferrosponges for controlled drug release. J Control Release 2007;121:181-9.
6. Liu TY, Hu SH, Liu KH, Liu DM, Chen SY. Study on controlled drug permeation of magnetic-sensitive ferrogels: effect of Fe_3O_4 and PVA. J Control Release 2008;126:228-36.
7. Müller-Schulte D, Schmitz-Rode T. Thermosensitive magnetic polymer particles as contactless controllable drug carriers. J Magnetism Magnetic Mater 2006;302:267-71.
8. Rahimi M, Yousef M, Cheng Y, Meletis EI, Eberhart RC, Nguyen K. Formulation and characterization of a covalently coated magnetic nanogel. J Nanosci Nanotechnol 2009;9:4128-34.
9. Arias JL, Ruiz MA, Gallardo V, Delgado AV. Tegafur loading and release properties of magnetite/poly(alkylcyanoacrylate) (core/shell) nanoparticles. J Control Release 2008;125:50-8.
10. Gupta AK, Curtis AS. Surface modified superparamagnetic nanoparticles for drug delivery: interaction studies with human fibroblasts in culture. J Mater Sci Mater Med 2004;15:493-6.
11. Zhang J, Misra RD. Magnetic drug-targeting carrier encapsulated with thermosensitive smart polymer: core-shell nanoparticle carrier and drug release response. Acta Biomater 2007;3:838-50.
12. Zhang JL, Srivastava RS, Misra RD. Core-shell magnetite nanoparticles surface encapsulated with smart stimuli-responsive polymer: synthesis, characterization, and LCST of viable drug-targeting delivery system. Langmuir 2007;23:6342-51.
13. Zintchenko A, Ogris M, Wagner E. Temperature dependent gene expression induced by PNIPAM-based copolymers: potential of hyperthermia in gene transfer. Bioconjug Chem 2006;17:766-72.
14. Chilkoti A, Dreher MR, Meyer DE, Raucher D. Targeted drug delivery by thermally responsive polymers. Adv Drug Deliv Rev 2002;54:613-30.
15. Meyer DE, Shin BC, Kong GA, Dewhirst MW, Chilkoti A. Drug targeting using thermally responsive polymers and local hyperthermia. J Control Release 2001;74:213-24.
16. Hu Z, Huang G. A new route to crystalline hydrogels, guided by a phase diagram. Angew Chem Int Ed Engl 2003;42:4799-802.

17. Rahimi M, Yousef M, Cheng Y, Meletis EI, Eberhart RC, Nguyen K. Formulation and characterization of novel temperature sensitive polymeric coated magnetic nanoparticles. J Nanosci Nanotechnol 2009;9:4128-34.
18. Rahimi M, Kilaru S, Hajj S, Ghida EL, Saleh A, Rudkevich D, et al. Synthesis and characterization of thermo-sensitive nanoparticles for drug delivery applications. J Biomed Nanotechnol 2008;4:1-9.
19. Doiron AL, Homan KA, Emelianov S, Brannon-Peppas L. Poly(lactic-co-glycolic) acid as a carrier for imaging contrast agents. Pharm Res 2009;26:674-82.
20. Yang J, Lee CH, Ko HJ, Suh JS, Yoon HG, Lee K, et al. Multifunctional magneto-polymeric nanohybrids for targeted detection and synergistic therapeutic effects on breast cancer. Angew Chem Int Ed Engl 2007;46: 8836-9.
21. Yu MK, Jeong YY, Park J, Park S, Kim JW, Min JJ, et al. Drug-loaded superparamagnetic iron oxide nanoparticles for combined cancer imaging and therapy in vivo. Angew Chem Int Ed Engl 2008;47: 5362-5.
22. Ramanan RM, Chellamuthu P, Tang L, Nguyen KT. Development of a temperature-sensitive composite hydrogel for drug delivery applications. Biotechnol Prog 2006;22:118-25.
23. Gupta AK, Gupta M. Cytotoxicity suppression and cellular uptake enhancement of surface modified magnetic nanoparticles. Biomaterials 2005;26:1565-73.
24. Nattama S, Rahimi M, Wadajkar AS, Koppolu B, Hua J, Nwariaku F, et al. Characterization of polymer coated magnetic nanoparticles for targeted treatment of cancer. Engineering in Medicine and Biology Workshop. Dallas, Texas: IEEE; 2007. p. 35-8. (doi:10.1109/EMBSW.2007.4454167).
25. Butoescu N, Jordan O, Burdet P, Stadelmann P, Petri-Fink A, Hoffmann H, et al. Dexamethasone-containing biodegradable superparamagnetic microparticles for intra-articular administration: physicochemical and magnetic properties, in vitro and in vivo drug release. Eur J Pharm Biopharm 2009;72:529-38.
26. Butoescu N, Seemayer CA, Foti M, Jordan O, Doelker E. Dexamethasone-containing PLGA superparamagnetic microparticles as carriers for the local treatment of arthritis. Biomaterials 2009;30: 1772-80.
27. Park SI, Lim JH, Hwang YH, Kim SM, Kim JH, Kim CG, et al. In vivo and in vitro antitumor activity of doxorubicin-loaded magnetic fluids. Phys Status Solidi 2007;4:4345-51.
28. Martin AL, Bernas LM, Rutt BK, Foster PJ, Gillies ER. Enhanced cell uptake of superparamagnetic iron oxide nanoparticles functionalized with dendritic guanidines. Bioconjug Chem 2008;19:2375-84.
29. Shen S, Liu Y, Huang P, Wang J. In vitro cellular uptake and effects of Fe_3O_4 magnetic nanoparticles on HeLa cells. J Nanosci Nanotechnol 2009;9:2866-71.
30. Villanueva A, Canete M, Roca AG, Calero M, Veintemillas-Verdaguer S, Serna CJ, et al. The influence of surface functionalization on the enhanced internalization of magnetic nanoparticles in cancer cells. Nanotechnology 2009;115103:20.
31. Arbab AS, Bashaw LA, Miller BR, Jordan EK, Lewis BK, Kalish H, et al. Characterization of biophysical and metabolic properties of cells labeled with superparamagnetic iron oxide nanoparticles and transfection agent for cellular MR imaging. Radiology 2003; 229:838-46.
32. Dodd SJ, Williams M, Suhan JP, Williams DS, Koretsky AP, Ho C. Detection of single mammalian cells by high-resolution magnetic resonance imaging. Biophys J 1999;76(Pt 1):103-9.
33. Frank JA, Miller BR, Arbab AS, Zywicke HA, Jordan EK, Lewis BK, et al. Clinically applicable labeling of mammalian and stem cells by combining superparamagnetic iron oxides and transfection agents. Radiology 2003;228:480-7.
34. Gupta AK, Naregalkar RR, Vaidya VD, Gupta M. Recent advances on surface engineering of magnetic iron oxide nanoparticles and their biomedical applications. Nanomedicine (Lond) 2007;2:23-39.
35. Alexiou C, Jurgons R, Seliger C, Iro H. Medical applications of magnetic nanoparticles. J Nanosci Nanotechnol 2006;6:2762-8.
36. Xiao X, He Q, Huang K. Possible magnetic multifunctional nanoplatforms in medicine. Med Hypotheses 2007;68:680-2.
37. Ito A, Shinkai M, Honda H, Kobayashi T. Medical application of functionalized magnetic nanoparticles. J Biosci Bioeng 2005;100:1-11.